

# Imaging morphodynamics of human blood cells *in vivo* with video-rate third harmonic generation microscopy

Chien-Kuo Chen<sup>1</sup> and Tzu-Ming Liu<sup>1,2\*</sup>

<sup>1</sup>*Institute of Biomedical Engineering, National Taiwan University, No.1, Sec. 4, Roosevelt Road, Taipei 10617, Taiwan*

<sup>2</sup>*Molecular Imaging Center, National Taiwan University, No.1, Sec. 4, Roosevelt Road, Taipei 10617, Taiwan*  
\*tmliu@ntu.edu.tw

**Abstract:** With a video-rate third harmonic generation (THG) microscopy system, we imaged the micro-circulation beneath the human skin without labeling. Not only the speed of circulation but also the morpho-hydrodynamics of blood cells can be analyzed. Lacking of nuclei, red blood cells (RBCs) shows typical parachute-like and hollow-core morphology under THG microscopy. Quite different from RBCs, every now and then, round and granule rich blood cells with strong THG contrast appear in circulation. The corresponding volume densities in blood, evaluated from their frequencies of appearance and the velocity of circulation, fall within the physiological range of human white blood cell counts.

© 2012 Optical Society of America

**OCIS codes:** (170.6900) Three-dimensional microscopy; (190.1900) Diagnostic applications of nonlinear optics.

## References and links

1. J. G. Fujimoto, M. E. Brezinski, G. J. Tearney, S. A. Boppart, B. Bouma, M. R. Hee, J. F. Southern, and E. A. Swanson, "Optical biopsy and imaging using optical coherence tomography," *Nat. Med.* **1**(9), 970–972 (1995).
2. M. Rajadhyaksha, S. González, J. M. Zavislan, R. R. Anderson, and R. H. Webb, "*In vivo* confocal scanning laser microscopy of human skin II: advances in instrumentation and comparison with histology," *J. Invest. Dermatol.* **113**(3), 293–303 (1999).
3. G. J. Tearney, R. H. Webb, and B. E. Bouma, "Spectrally encoded confocal microscopy," *Opt. Lett.* **23**(15), 1152–1154 (1998).
4. L. Golan, D. Yeheskely-Hayon, L. Minai, E. J. Dann, and D. Yelin, "Noninvasive imaging of flowing blood cells using label-free spectrally encoded flow cytometry," *Biomed. Opt. Express* **3**(6), 1455–1464 (2012).
5. L. Liu, J. A. Gardecki, S. K. Nadkarni, J. D. Toussaint, Y. Yagi, B. E. Bouma, and G. J. Tearney, "Imaging the subcellular structure of human coronary atherosclerosis using micro-optical coherence tomography," *Nat. Med.* **17**(8), 1010–1014 (2011).
6. K. König, A. Ehlers, F. Stracke, and I. Riemann, "*In vivo* drug screening in human skin using femtosecond laser multiphoton tomography," *Skin Pharmacol. Physiol.* **19**(2), 78–88 (2006).
7. J. Paoli, M. Smedh, A.-M. Wennberg, and M. B. Ericson, "Multiphoton laser scanning microscopy on non-melanoma skin cancer: morphologic features for future non-invasive diagnostics," *J. Invest. Dermatol.* **128**(5), 1248–1255 (2008).
8. S.-Y. Chen, S.-U. Chen, H.-Y. Wu, W.-J. Lee, Y.-H. Liao, and C.-K. Sun, "*In vivo* virtual biopsy of human skin by using noninvasive higher harmonic generation microscopy," *IEEE J. Sel. Top. Quantum Electron.* **16**(3), 478–492 (2010).
9. S.-Y. Chen, H.-Y. Wu, and C.-K. Sun, "*In vivo* harmonic generation biopsy of human skin," *J. Biomed. Opt.* **14**(6), 060505 (2009).
10. S.-H. Chia, C.-H. Yu, C.-H. Lin, N.-C. Cheng, T.-M. Liu, M.-C. Chan, I.-H. Chen, and C.-K. Sun, "Miniaturized video-rate epi-third-harmonic-generation fiber-microscope," *Opt. Express* **18**(16), 17382–17391 (2010).
11. M.-R. Tsai, S.-Y. Chen, D.-B. Shieh, P.-J. Lou, and C.-K. Sun, "*In vivo* optical virtual biopsy of human oral mucosa with harmonic generation microscopy," *Biomed. Opt. Express* **2**(8), 2317–2328 (2011).
12. B. G. Saar, C. W. Freudiger, J. Reichman, C. M. Stanley, G. R. Holtom, and X. S. Xie, "Video-rate molecular imaging *in vivo* with stimulated Raman scattering," *Science* **330**(6009), 1368–1370 (2010).
13. J. Squier, M. Muller, G. Brakenhoff, and K. R. Wilson, "Third harmonic generation microscopy," *Opt. Express* **3**(9), 315–324 (1998).
14. D. Yelin and Y. Silberberg, "Laser scanning third-harmonic-generation microscopy in biology," *Opt. Express* **5**(8), 169–175 (1999).

15. S.-W. Chu, S.-Y. Chen, T.-H. Tsai, T.-M. Liu, C.-Y. Lin, H.-J. Tsai, and C.-K. Sun, "In vivo developmental biology study using noninvasive multi-harmonic generation microscopy," *Opt. Express* **11**(23), 3093–3099 (2003).
16. N. Olivier, M. A. Luengo-Oroz, L. Duloquin, E. Faure, T. Savy, I. Veilleux, X. Solinas, D. Débarre, P. Bourguine, A. Santos, N. Peyri ras, and E. Beaufepaire, "Cell lineage reconstruction of early zebrafish embryos using label-free nonlinear microscopy," *Science* **329**(5994), 967–971 (2010).
17. D. Débarre, W. Supatto, A.-M. Pena, A. Fabre, T. Tordjmann, L. Combettes, M.-C. Schanne-Klein, and E. Beaufepaire, "Imaging lipid bodies in cells and tissues using third-harmonic generation microscopy," *Nat. Methods* **3**(1), 47–53 (2006).
18. R. D. Schaller, J. C. Johnson, and R. J. Saykally, "Nonlinear chemical imaging microscopy: near-field third harmonic generation imaging of human red blood cells," *Anal. Chem.* **72**(21), 5361–5364 (2000).
19. R. Skalak and P.-I. Branemark, "Deformation of red blood cells in capillaries," *Science* **164**(3880), 717–719 (1969).
20. B. Kaoui, G. Biros, and C. Misbah, "Why do red blood cells have asymmetric shapes even in a symmetric flow?" *Phys. Rev. Lett.* **103**(18), 188101 (2009).
21. D. Kobat, N. G. Horton, and C. Xu, "In vivo two-photon microscopy to 1.6-mm depth in mouse cortex," *J. Biomed. Opt.* **16**(10), 106014 (2011).
22. C.-K. Tsai, Y.-S. Chen, P.-C. Wu, T.-Y. Hsieh, H.-W. Liu, C.-Y. Yeh, W.-L. Lin, J.-S. Chia, and T.-M. Liu, "Imaging granularity of leukocytes with third harmonic generation microscopy," *Biomed. Opt. Express* **3**(9), 2234–2243 (2012).
23. S. S. Gorthi and E. Schonbrun, "Phase imaging flow cytometry using a focus-stack collecting microscope," *Opt. Lett.* **37**(4), 707–709 (2012).
24. M. N. Hart and A. G. Loeffler, *Introduction to Human Disease* (Jones & Bartlett Learning, 2012), pp 130.

## 1. Introduction

Virtual optical biopsy has emerged as a field of clinical diagnosis, through which a non-invasive sectioning microscopy image is taken *in vivo* to help investigating the physiological or pathological conditions of diseases [1]. Based on intrinsic scattering, absorption, and fluorescence contrasts of human tissues, many advanced *in vivo* optical microscopy tools for virtual biopsy have been developed. Using reflectance confocal microscopy [2], spectrally encoded confocal microscopy [3,4], micro-optical coherence tomography [5], and the nonlinear nature of multiphoton contrasts [6–12], cellular level resolution of virtual biopsy have been demonstrated in human. Among these modalities of virtual biopsy, third harmonic generation (THG) microscopy, due to the Gouy phase shift of focused Gaussian beam, can image the boundaries of optical heterogeneity without labeling [13,14]. Different from phase contrast or differential interference contrast (DIC) microscopes, the infrared excitation and third-order nonlinear nature of THG make THG microscopy a better modality to performed thick tissues or *in vivo* imaging with 3D sub-micron spatial resolution [8–11,15–17]. Compared with infrared excited reflectance confocal or spectrally encoded confocal microscopy, THG modality have better contrast and higher spatial resolution (<500 nm), which is critical for morphological [8,9,11,15] or morphodynamical [10,16,17] studies on cells *in vivo*. Not just a pure morphological imaging, THG contrasts can be resonantly enhanced by endogenous molecules like lipid [17], melanin [8,9], and hemoglobin [18]. These molecule-enhanced THG properties, in consequence, provide intrinsic contrast mechanisms that are necessary to visualize and resolve the nucleus, organelles, or morphologies of cells *in vivo* [8–11,14–16]. With these unique advantages, under the context of *in vivo* clinical microscopy, infrared femtosecond laser based THG microscopy is a least invasive, deep penetration depth, and labeling-free modality suitable for cell morphological diagnosis in superficial human tissues like skin [8,9] or mucosa [11].

Recently, using miniaturized THG microscope, a real-time flow of human red-blood-cells (RBCs) can be observed *in vivo* with a 3D sub-micron spatial resolution [10]. This preliminary result indicates a possibility of using THG microscopy for *in vivo* cytometry or hematology analysis without a draw of blood. To realize *in vivo* blood cytometry, here we employed video-rate (30 Hz) THG microscopy to analyze the microcirculation properties of capillaries beneath human skin. With improved contrast and length of recording time, we can observe and analyze the sub-cellular granules and morphodynamics of circulating blood cells in microcirculation. Different from parachute-shaped RBCs [19,20], we found round blood cells with bright THG contrast. Estimated from their frequency of appearance and the velocity

of circulation, the volume density of this round and bright THG-contrasted cells agrees with that of white blood cell counts for human under normal physiological conditions.

## 2. Imaging setup and imaging protocol

Figure 1 shows the schematic diagram of our home-build video-rate THG microscope. The laser light source used was a femtosecond Cr:forsterite laser. The 1250 nm operation wavelength falls in the infrared penetration window (1200-1300 nm) of most biological tissues. With least scattering and absorption attenuation, THG microscopy in thick (~1 mm) zebrafish embryo [15] or two-photon fluorescence imaging in deep (~1.6 mm) mouse cortex [21] have been demonstrated *in vivo*. Since the operation wavelength is far-away from the two-photon resonant excitation band of most endogenous fluorophores like NADH or flavins, deeper penetration depth and reduced on-focus photodamages can be achieved. The typical output power of our laser was 520 mW with a 110-MHz repetition rate and a 88fs pulse-width. In this work, to observe fast blood flow *in vivo*, a high-speed laser scanning rate is necessary. The 2-axis optical scanner (Electro-Optical Products) in the imaging system was composed of a 16 kHz resonant scanning mirror and a galvanometer mirror. With this scanner, the frame rate of a  $512 \times 512$  pixels image can easily be raised up to 30 frames per second (fps). The mirror size and the scanning optical angle of the resonant scanner were 3mm and 5 degree, respectively. Through a telescope ( $5 \times$ ) and a 45deg reflection dichroic beam splitter (DBS), the scanning laser beam was expanded to fill the back aperture of focusing objective (HCX APO, NA = 1.1,  $40 \times$  water immersion, Olympus) mounting on an inverted microscope (DMI 3000 M, Leica). The pivot point of xy scanning was thus imaged to the back focal plane of the objective, which resulted in a xy scanning of focused spot in human hands. The generated THG signals from tissues were epi-collected by the same objective and pass through a 690nm edged DBS. Then the THG signals (blue arrows) passed through a color glass filter (CGF), were detected by a photomultiplier tube (H7732-10, Hamamatsu), and amplified by a 50MHz bandwidth transimpedance amplifier (C6438-01, Hamamatsu). Finally, the THG signal stream were sampled, synchronized, and recombined to images with a high-speed frame grabber (Odyssey, Matrox) plug in a computer. Taking advantage of the video-rate scanning capability, our system can observe the motion and the morphology of blood cells in human blood capillary beneath skin.

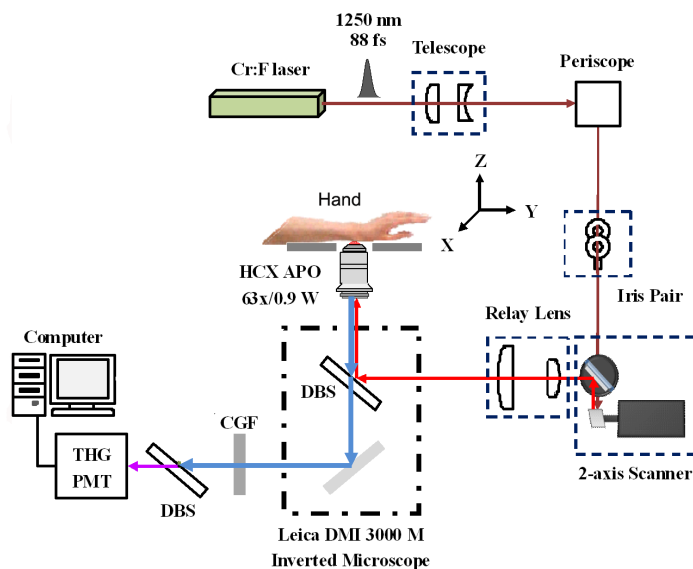


Fig. 1. The schematic diagram of the video-rate third harmonic generation (THG) microscopy system with a commercial inverted microscope (DMI 3000 M, Leica). DBS: Dichroic beam splitter; CGF: Colored glass filter; PMT: Photomultiplier tube.

The experimental protocol of human clinical trial on volunteers follows our previous works [8,9], and it was approved by the institutional review board (IRB) of National Taiwan University Hospital. Basically, volunteers put their dorsal part of forearm on the platform of the inverted microscope (as shown in Fig. 1). At center of the platform, we mount a transparent and thin glass window, on which the skin can be flatly contact. The distance between water immersion objective and the skin can thus be kept constant. The laser power after objective was below 90mW. Turning on the THG *in vivo* imaging system, we found the place of capillary beneath skin and record the flow of blood cells. The whole procedure, include recording and finding the capillaries, won't be longer than 15 minutes. It has been validated that this imaging protocol gives no significant injury on illuminated area of skin [8,9].

### 3. Results and discussions

Starting from the surface of human skin, as described in references [8,9], epidermis layer showed strong THG signals from keratinocytes. Moving the sectioning plane deeper into the junction between epidermis and dermis layers of skin, capillary loops (outlined by yellow dashed lines, Fig. 2(a)) can be found in dermal papilla (DP) region surrounded by basal cells (BC) (Fig. 2(a)). Basal cells have strong intracellular THG enhanced by melanin [8,9]. We tuned the depth of the imaging plane so that the sectioned capillaries have largest cross sections. Since the size of human red blood cells are typically  $8\mu\text{m}$ , within a  $85\mu\text{m} \times 85\mu\text{m}$  field of view, the time it took to scan through them were typically 3 millisecond. For  $300\mu\text{m}/\text{sec}$  circulation speed at deep vessel [10], blood cells only moved  $0.9\mu\text{m}$  in each frame, which wouldn't give severe distortion of images. In the course of 30fps recording, THG microscopy constantly captured the images of parachute-shaped RBCs (Fig. 2(a)), which is governed and can be predicted by hydrodynamic physics [20]. However, every now and then, we observed round blood cells with much brighter THG contrast than RBCs and surrounding basal cells (Fig. 2(b), pointed by a white arrow). Such bright THG contrast could originate from the densely-packed lipid granules inside the blood cells [22]. The round shape dose not satisfies the predicted hydrodynamic shapes of RBCs in confined circulation [20]. It looks more like white blood cells (WBCs) with nuclei, which maintain their round shapes in circulation [23].

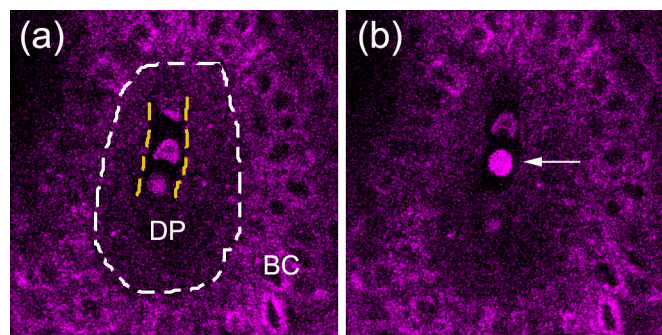


Fig. 2. (a) *In vivo* THG microscopy of human capillary (outlined by yellow dashed lines) in dermal papilla (DP) surrounded by basal cells (BC). Average vessel diameter is  $7.5\mu\text{m}$ . (b) Next few frames of THG images observed a round and bright blood cells (indicated with white arrows). Fields of view:  $85 \times 85\mu\text{m}$ .

Within 4-minutes of recording, in the capillary of a volunteer, we captured 15 round blood cells (Fig. 3). We analyzed consecutive frames of them to make sure they maintained round shapes in circulation. Cell number 12, shown in Fig. 2(b), was the brightest one. Other round cells more or less had one or two (number 6 and 8 in Fig. 3) dimmed THG regions within cells. Just like the negative contrast in basal cells (Fig. 2), they might be the signatures of nuclei. If this dimmed region indicates the nucleus of white blood cells, the number 7 round cell in Fig. 3 could be the lymphocyte with single large nucleus. When nuclei fall out of the sectioning

plane of THG images, just like cell number 12, dimed regions in cells might not be clear. These results showed the quality of contrast and resolution of video-rate THG microscopy on fast moving blood cells in deep tissues. We believe better resolution and contrast can be achieved with the help of adaptive optics. To estimate the volume density of these round cells, we measured the velocities of blood cells in capillary. Taking the round cell number 13 as an example, the cell traveled through the imaging plane within four frames (Figs. 4(a)–4d), indicated by white arrows). Obviously, the cell emerged beneath the imaging plane (Fig. 4(a)), traveled with similar size in following two frames (Figs. 4(b) and 4(c)), and finally dived beneath the imaging plane again (Fig. 4(d)). The blood cell that follows the round cell showed asymmetric slipper shape, which is also typical for red blood cells in confined circulation [20].

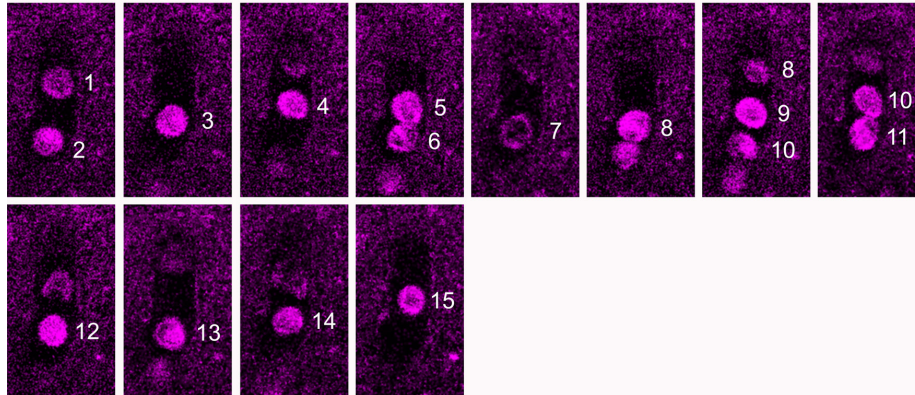


Fig. 3. *In vivo* THG images of 15 round blood cells captured within 4-minutes of recording in human capillary. Average diameter of human capillary is  $7.5 \mu\text{m}$ . Fields of view:  $24 \times 42 \mu\text{m}$ .

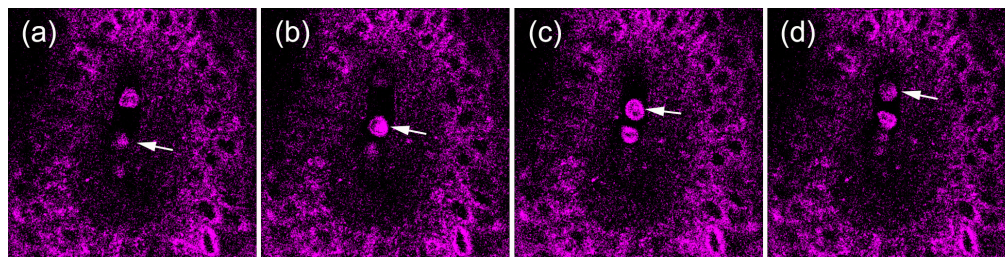


Fig. 4. Consecutive THG images of round blood cells moving in human blood capillary. Fields of view:  $85 \times 85 \mu\text{m}$ . The moving distance between (b) and (c) of round cell is  $5.89 \mu\text{m}$ .

The horizontally traveling distance between frame 2 and frame 3 was  $5.89 \mu\text{m}$ , which resulted in a  $176 \mu\text{m}/\text{sec}$  instantaneous velocity. This velocity in papilla capillary was slower than our previous result of  $300 \mu\text{m}/\text{sec}$  measured in deep vessel of dermis layer [10]. Measuring on more than 30 blood cells, the average velocity of blood flow in capillary was  $131 \pm 40 \mu\text{m}/\text{sec}$ . Considering a  $7.5\text{-}\mu\text{m}$  capillary diameter, the flux of blood within 4 minutes was  $1.39 \pm 0.42 \times 10^{-3} \text{ mm}^3$ . For 15 counts of round cells, the estimated volume density of round cells was  $10800 \pm 2527/\text{mm}^3$ . This average value falls in the range of typical white blood cell counts ( $4300\text{--}11600/\text{mm}^3$ ) for human in physiological conditions [24]. In another volunteer, we observed 7 round cells within 4minutes recording at a  $6.9\mu\text{m}$  sized capillary with a  $150 \pm 46 \mu\text{m}/\text{sec}$  average velocity of blood cells. The estimated volume density was  $5200 \pm 1211/\text{mm}^3$ , which is also within the range of white blood cell count. The large variation of round blood cell density between individuals could be due to not enough length of observation time. Density of blood cells might also depend on the size of capillary. Thus far, we believe these round cells, other than parachute-shaped red blood cells, are most likely

white blood cells. In order to specify the identities of round cells, more *in vitro* observations, longer recording time, and more comparison with blood tests are required.

#### **4. Conclusion**

In conclusion, using video-rate *in vivo* THG microscopy, we have successfully imaged the morphodynamics of human blood cells in subcutaneous capillaries. As described by conventional absorption bright-field microscopy [19], parachute- or slipper-shaped red blood cells can be constantly observed. Occasionally, we observed round blood cells with strong sub-cellular THG contrasts. These cells maintain their shapes when flowing through the imaging fields, which show quite different morphodynamics from those of RBCs. Estimated from their frequency of appearance and the average speed of blood flow, we found the volume density of these round blood cells fall within the physiological range of white blood cell counts of human. Whether round blood cells were WBCs requires further examination with more *in vitro* studies, longer image recording time, and more clinical trials on volunteers. Combined with adaptive optics and pattern recognition algorithms, we believe this *in vivo* THG cytometry of human blood cells is potential to be developed as a non-invasive hematology tool to analyze hydrodynamics of blood cells and perform whole blood counts on-site without a draw of blood.

#### **Acknowledgments**

This study is funded by National Science Council Taiwan under the grant number of NSC 100-2628-E-002-006 and by National Health Research Institutes under grant number of NHRI-EX101-9936EI.